JOINT EUROPEAN TORUS

JET–P(92)09

F.J. de Heer, R. Hoekstra, A.E. Kingston, H.P. Summers
and JET Team

Excitation of Neutral Helium by Electron Impact

Excitation of Neutral Helium by Electron Impact

F.J. de Heer[1], R. Hoekstra[2], A.E. Kingston[3], H.P. Summers[4]
and JET Team*

JET-Joint Undertaking, Culham Science Centre, OX14 3DB, Abingdon, UK

[1]FOM Institute for Atomic and Molecular Physics, Amsterdam, The Netherlands.
[2]K.V.I., Zemikelaan, Groningen, The Netherlands
[3]Department of Applied Mathematics, The Queen's University, Belfast
JET-Joint Undertaking, Culham Science Centre, OX14 3DB, Abingdon, UK
** See Annex*

Preprint of Paper to be submitted for publication in
Nuclear Fusion Supplement

ABSTRACT.

Experimental data for electron impact excitation of neutral helium in its ground state are reviewed critically. A preferred data set is established and combined with theoretical close coupling approximation data below the ionisation threshold and Born approximation data at high energy. Results are presented in tables and graphs. Maxwell averaged collision strengths are also tolerated

1. Introduction

A new assessment of electron impact cross-section data for excitation of helium from the 1 ^1S state is presented. This study was initiated with the expectation of the use of $^3He^\bullet$ and $^4He^\bullet$ neutral heating beams on the JET tokamak. It is now motivated and sustained by the actuality of their use in the 1991 experimental campaign. The resulting new observations of charge exchange spectra, beam emission spectra, thermal and recycling helium emission are of sufficient diagnostic quality to justify detailed atomic modelling of the effective emission and beam stopping processes. The studies are very relevant to the behaviour of slowing down alpha particles and helium ash in planned D/T fusion machines such as ITER and to beam based diagnostics of such plasmas.

Practically, the principal new contribution in this paper is the linkage of recent 29-state R-matrix calculations at low energies to reappraised experimental data at medium energies and on to the merging with asymptotic high energy behaviours.

The assessment of data presented here must be seen as a continuation and revision of previous compilations of experimental and theoretical data1)-4). The previous work also contains theoretical cross-sections for excitation from helium 2 ^1S and 2 ^3S metastable states. Compilation and analysis for the JET data base for the metastables is still in progress and will be reported in a later work.
The data is presented as figures and tables of collision strengths, Ω, and Maxwell averaged rate parameters, γ.

For a transition from an initial state i to a final higher excited state j,

$$\Omega_{ij} = w_i \left(\frac{E_i}{I_H} \right) \frac{\sigma_{i \to j}}{\pi a_0^2}$$

with w_i, the statistical weight of the initial state i of the atom, $\sigma_{i \to j}$, the excitation cross-section and E_i, the energy of the free projectile electron with the atom in the initial state i.

$$\gamma_{ij} = \int_0^\infty \Omega_{ij}(E_j)\, e^{-E_j/kTe}\, d(E_j / kT_e)$$

with E_j the energy of the free electron with the atom in the final state j and T_e the electron temperature. All other notation is conventional.

2. The theoretical data

Over the last ten years, the Queen's University group has conducted a series of R-matrix calculations of increasing complexity on neutral helium, culminating in the present 29 state study5). It is an LS coupled calculation including all 29 terms of the n=1 to 5 principal quantum shells. The successive calculations, for example 19 state and 29 state, show excellent convergence of the detailed resonance structure associated with the various n-shell series. This is illustrated in figure 1 for the $1\ ^1S - 2\ ^1S$ transition. However, since the calculations do not include a complete representation of the omitted higher states and continuum states, the results are in error near and above the ionisation threshold. This is analogous to that examined in detail for the H + e systems. Cross-sections above ionisation threshold (particularly for excitation to higher n-shells ≥3) may be overestimated by factors ≤2. The 29 state calculations have been executed at energies below ionisation threshold and are suitable for providing the low energy extension of the substantial body of experimental data which exists above ionisation threshold. In the present objectives, the R-matrix data is to be merged with experimental measurements of energy resolution less than that of the resonance structure and then quadratures performed over appropriate Maxwellian (or in some cases non-Maxwellian) distribution functions. It is therefore appropriate to form interval averages and it is these which are presented in the following tabulations and figures of collision strengths. Note also that adjustment is required for the differences between the theoretical bound state energies as used in the R-matrix codes and the exact observed energies. Conservatively, we have used R-matrix data up to the n=4 shell only, since the n=5 shell may be more strongly influenced by truncation.

At high energies, for non-spin changing transitions, the exact excitation cross-sections are expected to converge on those calculated in the first Born approximation. The accurate non-relativistic Born calculations of Bell et al. 6) are used to define the high energy limiting behaviour. Spin changing transitions are assumed to follow the $1/E^3$ behaviour suggested by Ochkur7). No precise high energy spin change calculations have been used in this work but simply extension of experimental data with the Ochkur slope.

3. The experimental data

The excitation cross sections of the JET data-base are based on experiment in the region of about 30 - 2000 eV electron impact energy for singlet excitation, merging into the theoretical first Born cross sections [6], and up to less high impact energies for triplet excitation, because the cross section becomes very small and, according to the the Ochkur approximation [7], decreases with the incident electron energy, E as E^{-3}. Below 30 eV an extrapolation is made towards the close coupling (29-states R-matrix) calculations [8] from threshold up to the ionization energy of He. Except for the metastable 2^1 S and 2 ^{3}S states, most experimental data are from photon emission cross section measurements reviewed by Heddle and Gallagher[9]. For metastables the (integrated) cross sections have been obtained by several groups by making use of their angular differential scattering cross sections for inelastic (energy loss selected) scattering of electrons (many of these data are reviewed by de Heer and Jansen [10]). Excitation of and cascade from ^{1,3} F levels has not been considered.

Typical for the experimental data is:

a) Similarity in the σ or Ω dependence on E in a term series where not too close to threshold. The cross section ratios at some sufficiently large E are equal to those in first order (Born) theory. (For high principal quantum number n, $\sigma(n^*) \sim n^{*-3}$ with n^* the effective principal quantum number)

b) At high energy, Ω becomes constant for non-spin changing optical forbidden transitions i.e. $1\,^1S - n\,^1S$ and $1\,^1S - n\,^1D$.

c) At high energies, $\Omega = \frac{4}{3} S_n \ln c_n E$ for optically allowed transitions, where c_n is a constant following from first Born theory and S_n is the optical line strength for the relevant $1\,^1S - n\,^1P$ transition.

d) At high energies cross sections for spin forbidden transitions, $1\,^1S - n\,^3L$, become very small, and should according to the Ochkur approximation decrease as E^{-3}.

e) The main maximum in the cross section is around 100 eV for n ^{1}P states, between 42 and 46 eV for n^1 D states, between 32 and 37 eV for n^1S states and between 26 and 30 eV for triplet states (see ref. 11).

The errors are generally smallest for singlet states (optical measurements) above about 40 eV, i.e. ~ 10%, and merge well into the theoretical Born cross sections between 500 and 2000 eV (dependent on the azimuthal quantum number ℓ) claimed within 5%. Only in the n^1 D states, is it necessary to choose a set of data different from Heddle and Gallagher [9)] above 1000e V in order to have a better fit with Born and therefore the error might not be 10%, but <30% there. At low energies, below 40eV the error may increase up to about 30%. For the 2 ^{1}S data (not optical) there is a problem. The cross section ratio, which is usually almost constant in a term series above about 50eV and equal to the Born ratio, increases for $\sigma(2\,^1S)/\sigma(3\,^1S)$ from 4.44 (Born at 1000 eV) to 5.98 (experiment at 100 eV). Therefore the 2 ^{1}S data towards 100 eV may be considered as an upper limit with an increased error up to ~30%. This accuracy may also persist to lower energies.

Errors in the triplet state cross sections are generally relatively large, because, in particular at high energies, secondary effects, like collisional transfers, are difficult to eliminate in experiment. The effect is largest for n^3 D states. The various theories (distorted waves, Born Oppenheimer, Ochkur etc.) sometimes give no unique results. Some experimental data were missing (i.e. for 3^3 S) or showed severe scatter (i.e. for 3^3 D) and were estimated via cross section ratios in the term series. Generally below 100 eV the error is ~30% for all triplet levels, although for 3^3 D it may be somewhat worse. Above 100eV there is an increasing uncertainty and our choice which often follows experiment, (deviating from $\sigma \sim E^{-3}$), may be considered somewhat arbitrary. More experimental and theoretical study and analysis is needed in this region. Because these cross sections become very small at high energies, the impact on the beam stopping and the beam diagnostics will be small.

4. Results and discussion

Table 1 summarises the primary choices of experimental data together with assessments of the accuracy of the cross-sections over the various energy intervals. Table 2 contains the interval averaged collision strengths from the 29-state R-matrix calculations. The averaging is over approximately 0.02 Rydbergs. Table 3 gives the assessed experimental data and table 4 presents the familiar Born results at high energy for completeness.

Figures 2a and 2b show the non-spin changing collision strengths from the 1 ^{1}S state. Figure 2a is of the low energy region up to 30eV giving the matching of experimental and R-matrix data. Figure 2b shows the region above 30eV, marking the experimental points, the preferred curves (solid lines) and the Born approximation (dotted). Figures 3a and 3b show the equivalent results for the spin changing collision strengths from 1 ^1S.

Table 5a and 5b give the Maxwell averaged collision strengths over an extended range of temperature. Since the detailed behaviour of the collision strength at threshold is not available, it has been assumed linear in the threshold energy to the first tabulated point. The uncertainty associated with this is estimated $\leq$ 20% at 1eV and $\leq$ 1% at 10eV. A correction is introduced for the integral from the last tabulated point to infinity according to the transition type.

REFERENCES

1. R K Janev, W D Langer, K Evans Jr., and D E Post Jr., Elementary processes in hydrogen-helium plasmas. Cross sections and reaction rates coefficients, 1987, Springer Verlag, Berlin, in particular pages 70-114 and 244-249.
2. T Fujimoto, IPPJ-AM-8, 1978, Semi-empirical cross sections and rate coefficients for excitation and ionization by electron collision and photoionization of helium, Institute of Plasma Physics, Nagoya University.
3. V A Abramov, L A Vainshtein, G I Krotova and A Yu Pigurov, INDC(CCP)-2861/GA, IAEA nuclear data section, 1988. Recommended atomic data for hydrogen and helium plasma. IAEA, Vienna.
4. B H Bransden and M R C McDowell, Physics reports 46, 250, 1979, Electron scattering at intermediate energies.
5. P M J Sawey, K A Berrington, P G Burke and A E Kingston, J. Phys. B Atom. Mol. Opt. Phys. 23, 4321, 1990.
6. K L Bell, D J Kennedy and A E Kingston, J Phys. B Atom Mol. Phys. 2,26, 1969.
7. V Ochkur, Sov. Phys. JETP 10, 503, 1964.
8. K A Berrington, M Sawey and A E Kingston private communication, 1991.
9. D W O Heddle and J W Gallagher, Rev. of Modern Physics, 61, 221, 1989.
10. F J de Heer and R H J Jansen, J Phys. B. Atom Mol. Phys. 10,3741, 1977.
11. I P Zapesochnyi, Astronomicheskii Zhurnal 43, 954, 1966.
12. S Trajmar, Phys. Rev. A8, 191, 1973.

13 R I Hall et al., J Physique 34, 827, 1973.

14 G B Crooks, Ph D Thesis 1972, University of Nebraska, Lincoln USA, G B Crooks, R D Dubois, D E Golden and M E Rudd, Phys Rev Lett 29, 327, 1972.

15. H H Brongersma, F W E Knoop and Backx, Chem Phys Lett, 13, 16, 1972
16. M A Dillon and E N Lassettre, J. Chem. Phys. 62, 2373, 1975.

17. A J F van Raan, J P de Jongh, J van Eck and H G M Heideman,
Physica 53, 45, 1971.
18. I P Zapesochnyi and P V Feltsan, UKr. Fiz Zh (Russ, Ed.), 10, 1197, 1965.
19. B van Zyl, G H Dunn, G Chamberlain and D W O Heddle,
Phys. Rev. A 22, 1916, 1980.
20. H R Moustafa Moussa, F J de Heer and J Schutten, Physica 40, 517, 1969
21. W B Westerveld, H G M Heideman and J van Eck, J Phys. B. Atom. Molec.
Phys. 12, 115, 1979.
22. J P de Jongh, Ph D Thesis, University of Utrecht, 1971,
Utrecht, The Netherlands.
J P de Jongh and J van Eck, ICPEAC Abstracts, 1971, P 701,
North Holland, Amsterdam.
23. D E Shemansky, J M Ajello, D T Hall and B Franklin,
Astrophys. Journal 296, 774, 1985.
24. F G Donaldson, M A Hender and J W McConkey,
J Phys B: Atom Molec. Phys. 5, 1192, 1972.
25. A J F van Raan, P G Moll and J van Eck,
J Phys B: Atom Molec Phys. 7,950, 1974
26. A R Johnston and P D Burrow J Phys. B: At. Mol. Phys.,
16, 613, 1983
27. J D Jobe and R M St. John, Phys Rev 164, 117, 1967
28. I P Bogdanova and S V Yurgenson, Opt. Spektrosk
61, 241, 1986.
29. A Chutjian and L D Thomas, Phys. Rev. 11, 1583, 1975.
30. J W McConkey and J M Woolsey,
ICPEAC VI abstracts, 1969, p.355, Ed I Amdur, MIT press.
31. J A Tully, J. Phys. B: At. Mol. Phys. 13, 4845, 1980.

Table 1a

$e + He(1\,^1S) \rightarrow e + He(n^1S)$

Excited State	Energy Range	Method	Reference	Accuracy
2^1 S	$\leq$ 24.58 eV	R-matrix 29-state close coupling.	Berrington[8]	< 10%
	30 $\leq$ E $\leq$ 100 eV	differential scattering integrated.	Trajmar[12] Hall[13] Crooks[14]	~ 30%
	23 eV	experiment retarding potential difference.	Brongersma[15]	~ 30%
	200 $\leq$ E $\leq$ 700 eV	differential scattering integrated.	Dillon[16]	30-10%
n^1 S (n=3,4,5,6)	$\leq$ 24.58 eV	R-matrix 29-state close coupling up to n=4.	Berrington[8]	< 10%
	< 50 eV	optical exp.	van Raan[17] Zapesochnyi[18] normalized	30-10 %
	50-2000 eV	optical exp. benchmark.	van Zyl[19] (Moustata Moussa)[20]	< 10%
	> 1000 eV	Born.	Bell[6]	< 5%

Table 1b

$e + He(1^1S) \rightarrow e + He\ (n^1P)$

Excited State	Energy Range	Method	Reference	Accuracy
n^1P ($n < 4$)	$\leq$ 24.58 eV	R-matrix 29-state close coupling	Berrington[8)]	< 10%
	30-2000 eV	optical exp.	Westerveld[21)]	< 10%
	> 500 eV	Born.	Bell[6)]	< 5%
4^1P	$\leq$ 24.58 eV	R-matrix 29 state close coupling	Berrington[8)]	< 10%
	40-3000 eV	optical exp.	de Jongh[22)] series III	< 10%
	> 500 eV	Born.	Bell[6)]	< 5%
n^1P, see also	all energies	optical exp. empirical analytical.	Shemansky[23)]	
	30-2000 eV	optical exp.	Donaldson[24)]	

Table 1c

$e + He(1^1S) \rightarrow e + He\,(n^1\,D)$

Excited State	Energy Range	Method	Reference	Accuracy
4^1D	$\leq$ 24.58 eV	R-matrix 29 state close coupling	Berrington[8]	< 10%
	50-100 eV	opt. exp.	Moustafa Moussa[20]	< 20%
	$\leq$ 50 eV	opt. exp.	Zapesochnyi[18] normalized van Raan[17]	~ 30%
	100-2000 eV	opt. exp.	van Raan[17] normalized	< 30%
	$\geq$ 2000 eV	Born.	Bell[6]	< 10%
5^1D	50-100 eV	opt. exp.	Moustafa Moussa[20]	<20%
	$\leq$ 50 eV	opt. exp.	Zapesochnyi[18] normalized van Raan[17]	~ 30%
	100-2000 eV	opt. exp.	van Raan[17] normalized	< 30%
	$\geq$ 2000 eV	Born.	Bell[6]	< 10%
3^1D	$\leq$ 24.58 eV	R-matrix 29 state close coupling	Berrington[8]	< 10%
	80-100 eV	opt. exp.	Moustafa Moussa[20] adjusted (/1.15)	< 20%
	50-80 eV	$\sigma(4\,^1D)/1.9$		< 20%
	$\leq$ 50 eV	opt. exp	Zaposochnyi[18] normalised	~ 30%
	100-2000 eV	$\sigma(4^1\,D)/1.82$		~ 30%
	$\geq$ 2000 eV	Born.	Bell[6]	< 10%
6^1D	$\leq$ 2000 eV	$\sigma(5^1\,D)/1.72$		~ 30%
	$\geq$ 2000 eV	Born	Bell[6]	< 10%

Table 1d

$e + He(1^1S) \rightarrow e + He\ (n^3S)$

Excited State	Energy Range	Method	Reference	Accuracy
$4\,^3S$	≤24.50 eV	R Matrix 29-state close coupling	Berrington[8]	< 10%
	25-100 eV	opt. exp.	van Raan[17]	~ 30%
	100-500 eV	opt. exp.	van Raan[25] adjusted (x1.15)	≥ 30 %
$2\,^3S$	< 24.58 eV	R-matrix 29-state close coupling.	Kingston[8]	< 10%
	20-100 eV	differential scattering integrated, retarding potential difference.	Trajmar[12] Hall[13] Crooks[14] Brongersma[15]	~ 30%
	≥ 100 eV	$\sigma\ (4\,^3S)/0.14$		uncertain
$3\,^3S$	< 24.58 eV	R-matrix 29-state close coupling.	Berrington[8]	< 10%
	all energies	interpolated between $\sigma\ (2\,^3S)$ and $\sigma\ (4^3S)$.		
	30 - 100 eV			~ 30%
	> 100 eV			uncertain

Note: Johnston and Burrow[26] in their electron trap experiment find the peak for 2^3S at 20.35 eV to be 6.2×10^{-18} cm^2.

Table 1e

e + He$(1^1S) \rightarrow e + He\ (n^3P)$

Excited State	Energy Range	Method	Reference	Accuracy
2^3P	≤ 24.50 eV	R-matrix 29-state close coupling.	Berrington$^{8)}$	< 10%
	30-100 eV	opt. exp. differential scattering integrated.	Jobe$^{27)}$, cascade corrected by de Heer 10$^{)}$ Trajmar$^{12)}$ Hall$^{13)}$ Crooks$^{14)}$	~ 30%
	> 100 eV	extrapolation $\sigma\ (2^3P) = 3.5x\ \sigma\ (3^3P)$		> 30%
3 ^{3}P	≤ 24.58 eV	R-matrix 29-state close coupling	Berrington$^{8)}$	< 10%
	≤ 40 eV	opt. exp.	Zapesochnyi$^{13)}$ normalized	~ 30%
	40-100 eV	opt. exp.	van Raan$^{17)}$	~ 30%
	100-1500 eV	opt. exp.	van Raan$^{25)}$ adjusted (x1.58)	> 30%

Note: not analysed data of Bogdanova and Yurgenson$^{28)}$, and of Chutjian and Thomas$^{29)}$.

Table 1f
4
e + He(1^1S) → *e + He* (n^3D)

Excited State	Energy Range	Method	Reference	Accuracy
4 ^{3}D	≤ 24.50 eV	R-matrix 29-state close coupling	Berrington[8)]	< 10%
	25-35 eV	opt. exp.	Zapesochnyi[18)] normalized	~ 30%
	35-100 eV	opt. exp.	Mc Conkey[30)]	~ 30%
	100-1000 eV	opt. exp.	van Raan[25)] normalized	> 30%
3^3D	≤ 24.58 eV	R-matrix 29-state close coupling	Berrington[8)]	< 10%
	< 100 eV	$\sigma(3^3D) = 2\,\sigma(4^3D)$		~ factor 2
	100-1000 eV	$\sigma(3^3D) = 2\,\sigma(4^3D)$		≥ factor 2

Note: For 3^3 D see also the theoretical work of Tully[31)].

Table 2a

29-state R-matrix 1 ^{1}S - n ^{1}S interval averaged collision strengths

E(eV)	2 ^{1}S	E(eV)	3 ^{1}S	E(eV)	4 ^{1}S
2.08^{1}	2.23^{-2}	2.31^{1}	9.29^{-3}	2.38^{1}	3.22^{-3}
2.11^{1}	4.22^{-2}	2.34^{1}	8.01^{-3}	2.40^{1}	2.02^{-3}
2.13^{1}	4.06^{-2}	2.37^{1}	8.54^{-3}	2.43^{1}	1.76^{-3}
2.16^{1}	4.09^{-2}	2.40^{1}	8.19^{-3}		
2.19^{1}	4.24^{-2}	2.41^{1}	7.76^{-3}		
2.22^{1}	4.30^{-2}	2.44^{1}	7.41^{-3}		
2.25^{1}	4.27^{-2}				
2.28^{1}	4.53^{-2}				
2.31^{1}	4.24^{-2}				
2.34^{1}	4.24^{-2}				
2.37^{1}	4.32^{-2}				
2.39^{1}	4.35^{-2}				
2.42^{1}	4.51^{-2}				
2.45^{1}	4.51^{-2}				

Table 2b

29-state R-matrix 1 ^{1}S - n ^{1}P interval averaged collision strengths

E(eV)	2 ^{1}P	E(eV)	3 ^{1}P	E(eV)	4 ^{1}P
2.13^{1}	4.64^{-3}	2.32^{1}	1.00^{-3}	2.39^{1}	4.03^{-4}
2.17^{1}	1.10^{-2}	2.36^{1}	2.42^{-3}	2.41^{1}	6.71^{-4}
2.19^{1}	1.54^{-2}	2.38^{1}	3.48^{-3}	2.43^{1}	1.07^{-3}
2.22^{1}	2.03^{-2}	2.40^{1}	4.37^{-3}		
2.25^{1}	2.63^{-2}	2.43^{1}	4.87^{-3}		
2.28^{1}	2.35^{-2}				
2.31^{1}	2.56^{-2}				
2.34^{1}	2.50^{-2}				
2.37^{1}	2.91^{-2}				
2.40^{1}	3.05^{-2}				
2.42^{1}	3.31^{-2}				
2.45^{1}	3.56^{-2}				

Table 2c

29-state R-matrix 1 ^{1}S - n ^{1}D interval averaged collision strengths

E(eV)	3 ^{1}D	E(eV)	4 ^{1}D
2.32^{1}	5.12^{-3}	2.39^{1}	1.88^{-3}
2.36^{1}	5.77^{-3}	2.41^{1}	1.50^{-3}
2.38^{1}	4.31^{-3}	2.43^{1}	1.33^{-3}
2.40^{1}	4.14^{-3}		
2.43^{1}	3.69^{-3}		

Table 2d

29-state R-matrix 1 ^{1}S - n ^{3}S interval averaged collision strengths

E(eV)	2 ^{3}S	E(eV)	3 ^{3}S	E(eV)	4 ^{3}S
2.00^{1}	6.27^{-2}	2.30^{1}	1.72^{-2}	2.37^{1}	6.23^{-3}
2.03^{1}	9.67^{-2}	2.32^{1}	1.67^{-2}	2.40^{1}	5.06^{-3}
2.06^{1}	7.80^{-2}	2.36^{1}	1.53^{-2}	2.43^{1}	4.00^{-3}
2.09^{1}	7.40^{-2}	2.38^{1}	1.43^{-2}		
2.12^{1}	7.21^{-2}	2.41^{1}	1.47^{-2}		
2.15^{1}	6.11^{-2}	2.43^{1}	1.34^{-2}		
2.18^{1}	6.02^{-2}				
2.21^{1}	6.06^{-2}				
2.24^{1}	6.04^{-2}				
2.26^{1}	6.68^{-2}				
2.29^{1}	5.88^{-2}				
2.32^{1}	5.87^{-2}				
2.35^{1}	5.76^{-2}				
2.38^{1}	5.84^{-2}				
2.41^{1}	5.75^{-2}				
2.43^{1}	5.98^{-2}				
2.46^{1}	5.78^{-2}				

Table 2e

29-state R-matrix 1 ^1S - n ^3P interval averaged collision strengths

E(eV)	2 ^3P	E(eV)	3 ^3P	E(eV)	4 ^3P
2.11^{1}	9.07^{-3}	2.31^{1}	5.73^{-3}	2.38^{1}	2.25^{-3}
2.14^{1}	1.87^{-2}	2.35^{1}	6.59^{-3}	2.40^{1}	2.14^{-3}
2.17^{1}	2.29^{-2}	2.37^{1}	7.58^{-3}	2.43^{1}	2.41^{-3}
2.19^{1}	2.69^{-2}	2.40^{1}	8.12^{-3}		
2.22^{1}	3.18^{-2}	2.43^{1}	8.48^{-3}		
2.26^{1}	3.84^{-2}				
2.28^{1}	3.70^{-2}				
2.31^{1}	3.93^{-2}				
2.34^{1}	3.79^{-2}				
2.38^{1}	4.21^{-2}				
2.40^{1}	4.21^{-2}				
2.42^{1}	4.46^{-2}				
2.45^{1}	4.66^{-2}				

Table 2f

29-state R-matrix 1 ^1S - n ^3D interval averaged collision strengths

E(eV)	3 ^3D	E(eV)	4 ^3D
2.32^{1}	1.45^{-3}	2.39^{1}	9.85^{-4}
2.36^{1}	4.10^{-3}	2.41^{1}	6.79^{-4}
2.38^{1}	2.12^{-3}	2.43^{1}	6.33^{-4}
2.40^{1}	2.01^{-3}		
2.43^{1}	1.80^{-3}		

Table 3a

Experimental 1 ^1S - n ^1S collision strengths and collision strength ratios of (n)/(n + 1)

E(eV)	2 ^1S	(2)/(3)	3 ^1S	(3)/(4)	4 ^1S	(4)/(5)	5 ^1S	(5)/(6)	6 ^1S
2.30^{1}	3.36^{-2}								
2.50^{1}			6.06^{-3}	2.67	2.28^{-3}	2.66	8.56^{-4}	2.16	3.97^{-4}
3.00^{1}	6.02^{-2}	6.13	9.80^{-3}	2.41	4.06^{-3}	2.31	1.76^{-3}	1.95	9.02^{-4}
3.50^{1}			1.20^{-2}	2.48	4.83^{-3}	2.18	2.21^{-3}	1.91	1.16^{-3}
4.00^{1}	7.05^{-2}	5.34	1.32^{-2}	2.50	5.08^{-3}	2.12	2.40^{-3}	1.89	1.27^{-3}
4.50^{1}					5.38^{-3}	2.10	2.56^{-3}		
5.00^{1}	8.10^{-2}	5.75	1.41^{-2}	2.53	5.56^{-3}	2.07	2.68^{-3}	1.89	1.42^{-3}
6.00^{1}	8.87^{-2}				5.66^{-3}	2.14	2.65^{-3}	1.88	1.42^{-3}
8.00^{1}	1.00^{-1}	5.74	1.74^{-2}	2.74	6.36^{-3}	2.22	2.86^{-3}	1.88	1.55^{-3}
1.00^{2}	1.09^{-1}	5.79	1.95^{-2}	2.57	7.57^{-3}	2.46	3.50^{-3}*	1.88	1.86^{-3}
1.50^{2}	1.29^{-1}	5.98	2.16^{-2}	2.46	8.76^{-3}	2.12	4.14^{-3}	1.98	2.08^{-3}
2.00^{2}	1.40^{-1}	5.75	2.44^{-2}	2.46	9.89^{-3}	2.11	4.70^{-3}	2.01	2.34^{-3}
2.50^{2}			2.74^{-2}	2.51	1.09^{-2}	2.09	5.22^{-3}	1.90	2.74^{-3}
3.00^{2}	1.59^{-1}	5.31	2.98^{-2}	2.63	1.13^{-2}	1.96	5.79^{-3}	1.98	2.93^{-3}
3.50^{2}			3.01^{-2}	2.56	1.18^{-2}	1.97	5.99^{-3}	1.95	3.07^{-3}
4.00^{2}	1.64^{-1}	5.34	3.06^{-2}	2.53	1.21^{-2}	1.97	6.15^{-3}	1.93	3.18^{-3}
5.00^{2}	1.77^{-1}	5.00	3.53^{-2}	2.59	1.36^{-2}	2.06	6.60^{-3}	1.86	3.55^{-3}
6.00^{2}	1.62^{-1}	4.79	3.39^{-2}	2.57	1.32^{-2}	1.94	6.82^{-3}	1.82	3.74^{-3}
8.00^{2}	1.79^{-1}	4.68	3.82^{-2}	2.53	1.51^{-2}	2.15	7.02^{-3}	1.88	3.74^{-3}
1.00^{3}	1.81^{-1}	4.68	3.87^{-2}	2.63	1.47^{-2}	2.04	7.20^{-3}	1.80	4.00^{-3}
1.50^{3}			3.94^{-2}	2.66	1.48^{-2}	1.96	7.56^{-3}	1.82	4.16^{-3}
2.00^{3}			4.09^{-2}	2.70	1.51^{-2}	2.02	7.47^{-3}	1.86	4.03^{-3}

* benchmark adjusted

Table 3b

Experimental 1 ^{1}S - n ^{1}P collision strengths and collision strength ratios of (n)/(n+1)

E(eV)	2 ^{1}P	(2)/(3)	3 ^{1}P	(3)/(4)	4 ^{1}P
3.00^{1}	9.40^{-2}	5.07	1.85^{-2}	2.39	7.77^{-3}◇
3.20^{1}	1.18^{-1}	4.66	2.54^{-2}		
3.50^{1}	1.59^{-1}	4.89	3.25^{-2}		
4.00^{1}	2.15^{-1}	4.66	4.61^{-2}	2.36	1.96^{-2}
4.50^{1}	2.90^{-1}	4.64	6.24^{-2}		
5.00^{1}	3.43^{-1}	4.46	7.69^{-2}	2.21	3.48^{-2}
6.00^{1}	4.77^{-1}	4.40	1.08^{-1}	2.30	4.73^{-2}
7.00^{1}	5.71^{-1}	4.18	1.37^{-1}		
8.00^{1}	6.78^{-1}	4.18	1.62^{-1}	2.11	7.69^{-2}
9.00^{1}	7.66^{-1}	4.16	1.84^{-1}		
1.00^{2}	8.44^{-1}	4.14	2.04^{-1}	2.28	8.94^{-2}
1.20^{2}	9.66^{-1}	3.99	2.42^{-1}		
1.50^{2}	1.15^{0}	4.06	2.83^{-1}	2.22	1.28^{-1}
1.80^{2}	1.32^{0}	4.00	3.31^{-1}		
2.00^{2}	1.39^{0}	3.99	3.48^{-1}	2.33	1.49^{-1}
2.50^{2}	1.59^{0}	4.06	3.93^{-1}		
3.00^{2}	1.74^{0}	3.93	4.44^{-1}	2.45	1.81^{-1}
3.50^{2}	1.87^{0}	3.93	4.77^{-1}		
4.00^{2}	1.99^{0}	3.93	5.05^{-1}	2.46	2.05^{-1}
5.00^{2}	2.37^{0} +	4.40	5.39^{-1}	2.44	2.21^{-1}
6.00^{2}	2.32^{0} *	4.17	5.56^{-1}*	2.33	2.39^{-1}*
8.00^{2}	2.51^{0} *	4.10	6.12^{-1}*	2.42	2.53^{-1}*
1.00^{3}	2.62^{0}	3.96	6.63^{-1}	2.48	2.67^{-1}
1.50^{3}	2.93^{0}	3.98	7.37^{-1}	2.53	2.91^{-1}
2.00^{3}	3.09^{0}	3.95	7.82^{-1}	2.46	3.18^{-1}

◇ Donaldson et al. 1972

* de Jongh & van Eck, VII ICPEAC 1971 Amsterdam

+ too high

Table 3c

Experimental 1 ^{1}S- n ^{1}D collision strengths and collision strength ratios of (n)/(n + 1)

E(eV)	3 ^{1}D	(3)/(4)	4 ^{1}D	(4)/(5)	5 ^{1}D	(5)/(6)	6 ^{1}D
2.50^{1}	4.01^{-3}	1.83	2.19^{-3}	1.71	1.28^{-3}	1.72	7.44^{-4}
3.00^{1}	5.72^{-3}	1.87	3.06^{-3}	1.69	1.80^{-3}	1.72	1.05^{-3}
3.50^{1}	7.25^{-3}	1.85	3.92^{-3}	1.64	2.39^{-3}	1.72	1.39^{-3}
4.00^{1}	8.66^{-3}	1.86	4.65^{-3}	1.68	2.76^{-3}	1.72	1.60^{-3}
4.50^{1}	9.93^{-3}	1.90	5.23^{-3}	1.73	3.02^{-3}	1.72	1.76^{-3}
5.00^{1}	1.09^{-2}	1.90	5.77^{-3}	1.86	3.10^{-3}	1.72	1.80^{-3}
6.00^{1}	1.14^{-2}	1.90	6.02^{-3}	1.86	3.23^{-3}	1.72	1.87^{-3}
8.00^{1}	1.24^{-2}	1.89	6.58^{-3}	1.81	3.54^{-3}	1.72	2.06^{-3}
1.00^{2}	1.20^{-2}	1.82	6.61^{-3}	1.87	3.53^{-3}	1.72	2.05^{-3}
1.50^{2}	1.17^{-2}	1.82	6.45^{-3}	1.87	3.46^{-3}	1.72	2.01^{-3}
2.00^{2}	1.18^{-2}	1.82	6.48^{-3}	1.87	3.48^{-3}	1.72	2.02^{-3}
2.50^{2}	1.21^{-2}	1.82	6.64^{-3}	1.87			
3.00^{2}	1.12^{-2}	1.82	6.17^{-3}	1.82	3.38^{-3}	1.72	1.97^{-3}
4.00^{2}	1.07^{-2}	1.82	5.88^{-3}	1.77	3.33^{-3}	1.72	1.94^{-3}
5.00^{2}	1.01^{-2}	1.82	5.56^{-3}	1.77			
6.00^{2}	1.00^{-2}	1.82	5.51^{-3}	1.74	3.17^{-3}	1.72	1.80^{-3}
8.00^{2}	1.04^{-2}	1.82	5.72^{-3}	1.84	3.10^{-3}	1.72	1.80^{-3}
1.00^{3}	1.04^{-2}	1.82	5.73^{-3}	1.83	3.12^{-3}	1.72	1.81^{-3}
1.50^{3}	9.78^{-3}	1.82	5.38^{-3}	1.83	2.93^{-3}	1.72	1.70^{-3}
2.00^{3}	9.73^{-3}	1.82	5.35^{-3}	1.83	2.91^{-3}	1.72	1.69^{-3}

Table 3d

Experimental 1 ^1S - n ^3S collision strengths and collision strength ratios of (n)/(n + 1)

E(eV)	2 ^3S	(2)/(3)	3 ^3S	(2)/(4)	4 ^3S
2.00^{1}	5.18^{-2}				
2.50^{1}	4.80^{-2}	3.29	1.46^{-2}	7.30	6.60^{-3}
3.00^{1}	4.76^{-2}	2.82	1.65^{-2}	6.25	7.67^{-3}
3.50^{1}	4.24^{-2}	2.41	1.75^{-2}	5.88	7.43^{-3}
4.00^{1}	3.94^{-2}	2.41	1.64^{-2}	5.88	6.65^{-3}
4.50^{1}	3.50^{-2}	2.82	1.24^{-2}	6.25	5.75^{-3}
5.00^{1}	3.09^{-2}	2.82	1.09^{-2}	6.25	4.93^{-3}
6.00^{1}	2.46^{-2}	3.01	8.02^{-3}	6.66	3.72^{-3}
7.00^{1}	2.05^{-2}	3.29	6.43^{-3}	7.14	2.92^{-3}
8.00^{1}	1.74^{-2}	3.29	5.28^{-3}	7.14	2.43^{-3}
9.00^{1}	1.35^{-2}	3.29	4.14^{-3}	7.14	1.88^{-3}
1.00^{2}	1.17^{-2}	3.29	3.51^{-3}	7.69	1.57^{-3}
1.50^{2}	5.89^{-3*}	3.29	1.75^{-3}	7.14	8.21^{-4}
2.00^{2}	4.01^{-3*}	3.29	1.20^{-3}	7.14	5.65^{-4}
2.50^{2}	2.92^{-3*}	3.29	8.77^{-4}	7.14	4.07^{-4}
3.00^{2}	2.28^{-3*}	3.29	6.77^{-4}	7.14	3.18^{-4}
4.00^{2}	1.54^{-3*}	3.29	4.68^{-4}	7.14	2.17^{-4}
5.00^{2}	1.04^{-3*}	3.29	3.13^{-4}	7.14	1.45^{-4}

For 2 ^3S, Johnston & Burrow [27)] have a peak in the cross-section at 20.35eV

* 7.14Ω(4 ^3S)

Table 3e

Experimental 1 ^1S - n ^3P collision strengths and collision strength ratios of (n)/(n + 1)

E(eV)	2 ^3P	(2)/(3)	3 ^3P
2.50^{1}			1.31^{-2}
3.00^{1}	6.52^{-2}	3.52	1.85^{-2}
3.50^{1}			1.84^{-2}
4.00^{1}	6.35^{-2}	3.58	1.77^{-2}
5.00^{1}	5.85^{-2}	3.65	1.60^{-2}
6.00^{1}	5.16^{-2}	3.86	1.34^{-2}
7.00^{1}	4.09^{-2}	3.62	1.13^{-2}
8.00^{1}	3.28^{-2}	3.45	9.49^{-3}
9.00^{1}	2.63^{-2}	3.30	7.97^{-3}
1.00^{2}	2.34^{-2}	3.46	6.81^{-3}
1.50^{2}	9.65^{-3}	3.5	2.76^{-3}
2.00^{2}	6.02^{-3}	3.5	1.70^{-3}
2.50^{2}	4.18^{-3}	3.5	1.19^{-3}
3.00^{2}	2.76^{-3}	3.5	8.02^{-4}
4.00^{2}	1.47^{-3}	3.5	4.18^{-4}
5.00^{2}	7.94^{-4}	3.5	2.21^{-4}
6.00^{2}	1.25^{-3}	3.5	3.51^{-4}
8.00^{2}	4.68^{-4}	3.5	1.34^{-4}
1.00^{3}	9.19^{-4}	3.5	2.51^{-4}

Table 3f

Experimental 1 ^1S - n ^3D collision strengths and collision strength ratios of (n)/(n + 1)

E(eV)	3 ^3D	(3)/(4)	4 ^3D
2.80^{1}	2.76^{-3}	2.0	1.38^{-3}
3.00^{1}	4.26^{-3}	2.0	2.13^{-3}
3.50^{1}	3.98^{-3}	2.0	1.99^{-3}
4.00^{1}	3.28^{-3}	2.0	1.64^{-3}
5.00^{1}	2.13^{-3}	2.0	1.06^{-3}
6.00^{1}	1.55^{-3}	2.0	7.77^{-4}
7.00^{1}	1.29^{-3}	2.0	6.43^{-4}
8.00^{1}	1.02^{-3}	2.0	5.08^{-4}
9.00^{1}	9.32^{-4}	2.0	4.66^{-4}
1.00^{2}	8.36^{-4}	2.0	4.18^{-4}
1.50^{2}	4.26^{-4}	2.0	2.13^{-4}
2.00^{2}	2.67^{-4}	2.0	1.30^{-4}
2.50^{2}	1.86^{-4}	2.0	9.19^{-5}
4.00^{2}	1.67^{-4}	2.0	9.02^{-5}
6.00^{2}	2.00^{-4}	2.0	9.53^{-5}
1.00^{3}	2.00^{-4}	2.0	1.00^{-5}

Table 4a

Born approx. $1\,^1S$ - $n\,^1S$ collision strengths and collision strength ratios of (n)/(n + 1)

E(eV)	$2\,^1S$	(2)/(3)	$3\,^1S$	(3)/(4)	$4\,^1S$
1.00^3	1.80^{-1}	4.44	4.05^{-2}	2.61	1.55^{-2}
1.50^3	1.80^{-1}	4.44	4.06^{-2}	2.61	1.56^{-2}
2.00^3	1.81^{-1}	4.44	4.07^{-2}	2.61	1.56^{-2}
3.00^3	1.81^{-1}	4.44	4.08^{-2}	2.61	1.56^{-2}
4.00^3	1.81^{-1}	4.44	4.08^{-2}	2.61	1.56^{-2}
5.00^3	1.81^{-1}	4.44	4.08^{-2}	2.61	1.56^{-2}

Table 4b

Born approx. $1\,^1S$ - $n\,^1P$ collision strengths and collision strength ratios of (n)/(n + 1)

E(eV)	$2\,^1P$	(2)/(3)	$3\,^1P$	(3)/(4)	$4\,^1P$
7.00^2	2.45^0	4.05	6.05^{-1}	2.49	2.43^{-1}
1.00^3	2.70^0	4.05	6.67^{-1}	2.49	2.67^{-1}
1.50^3	2.99^0	4.05	7.37^{-1}	2.49	2.95^{-1}
2.00^3	3.19^0	4.06	7.87^{-1}	2.49	3.15^{-1}
3.00^3	3.48^0	4.06	8.57^{-1}	2.49	3.43^{-1}
5.00^3	3.84^0	4.06	9.45^{-1}	2.50	3.79^{-1}

Table 4c

Born approx. $1\,^1S$ - $n\,^1D$ collision strengths and collision strength ratios of (n)/(n + 1)

E(eV)	$3\,^1D$	(3)/(4)	$4\,^1D$
1.00^3	9.42^{-3}	1.88	5.01^{-3}
1.50^3	9.49^{-3}	1.88	5.05^{-3}
2.00^3	9.53^{-3}	1.88	5.08^{-3}
3.00^3	9.56^{-3}	1.88	5.09^{-3}
4.00^3	9.58^{-3}	1.88	5.11^{-3}
5.00^3	9.59^{-3}	1.88	5.10^{-3}

Table 5a

Maxwell averaged 1 ^1S - n ^1L collision strengths

T(eV)	2 ^1S	3 ^1S	4 ^1S	3 ^1D	4 ^1D	2 ^1P	3 ^1P	4 ^1P
1.00^{0}	3.30^{-2}	6.69^{-3}	2.02^{-3}	4.11^{-3}	1.61^{-3}	1.64^{-2}	3.79^{-3}	1.48^{-3}
2.00^{0}	3.86^{-2}	7.01^{-3}	2.42^{-3}	4.32^{-3}	2.00^{-3}	2.61^{-2}	6.47^{-3}	2.70^{-3}
3.00^{0}	4.19^{-2}	7.13^{-3}	2.73^{-3}	4.58^{-3}	2.26^{-3}	3.62^{-2}	9.09^{-3}	3.90^{-3}
4.00^{0}	4.45^{-2}	7.21^{-3}	2.99^{-3}	4.86^{-3}	2.48^{-3}	4.68^{-2}	1.17^{-2}	5.11^{-3}
5.00^{0}	4.67^{-2}	7.32^{-3}	3.21^{-3}	5.13^{-3}	2.67^{-3}	5.78^{-2}	1.44^{-2}	6.33^{-3}
7.00^{0}	5.04^{-2}	7.64^{-3}	3.55^{-3}	5.67^{-3}	3.00^{-3}	8.07^{-2}	1.99^{-2}	8.84^{-3}
1.00^{1}	5.05^{-2}	8.30^{-3}	3.92^{-3}	6.38^{-3}	3.41^{-3}	1.16^{-1}	2.84^{-2}	1.27^{-2}
1.50^{1}	6.11^{-2}	9.43^{-3}	4.35^{-3}	7.30^{-3}	3.92^{-3}	1.74^{-1}	4.24^{-2}	1.91^{-2}
2.00^{1}	6.61^{-2}	1.04^{-2}	4.67^{-3}	7.99^{-3}	4.29^{-3}	2.30^{-1}	5.60^{-2}	2.53^{-2}
3.00^{1}	7.40^{-2}	1.21^{-2}	5.18^{-3}	8.91^{-3}	4.80^{-3}	3.32^{-1}	8.12^{-2}	3.67^{-2}
4.00^{1}	8.04^{-2}	1.34^{-2}	5.60^{-3}	9.49^{-3}	5.12^{-3}	4.22^{-1}	1.04^{-1}	4.66^{-2}
5.00^{1}	8.59^{-2}	1.45^{-2}	5.97^{-3}	9.88^{-3}	5.33^{-3}	5.03^{-1}	1.24^{-1}	5.54^{-2}
7.00^{1}	9.48^{-2}	1.62^{-2}	6.60^{-3}	1.04^{-2}	5.61^{-3}	6.43^{-1}	1.60^{-1}	7.04^{-2}
1.00^{2}	1.05^{-1}	1.83^{-2}	7.35^{-3}	1.07^{-2}	5.82^{-3}	8.16^{-1}	2.03^{-1}	8.83^{-2}
1.50^{2}	1.17^{-1}	2.08^{-2}	8.31^{-3}	1.09^{-2}	5.95^{-3}	1.04^{0}	2.59^{-1}	1.11^{-1}
2.00^{2}	1.25^{-1}	2.28^{-2}	9.05^{-3}	1.10^{-2}	5.98^{-3}	1.22^{0}	3.02^{-1}	1.28^{-1}
3.00^{2}	1.37^{-1}	2.57^{-2}	1.01^{-2}	1.09^{-2}	5.97^{-3}	1.48^{0}	3.65^{-1}	1.53^{-1}
4.00^{2}	1.44^{-1}	2.77^{-2}	1.08^{-2}	1.08^{-2}	5.93^{-3}	1.67^{0}	4.12^{-1}	1.72^{-1}
5.00^{2}	1.49^{-1}	2.92^{-2}	1.14^{-2}	1.07^{-2}	5.88^{-3}	1.81^{0}	4.48^{-1}	1.86^{-1}
7.00^{2}	1.56^{-1}	3.13^{-2}	1.22^{-2}	1.06^{-2}	5.80^{-3}	2.04^{0}	5.05^{-1}	2.08^{-1}
1.00^{3}	1.62^{-1}	3.33^{-2}	1.29^{-2}	1.04^{-2}	5.71^{-3}	2.28^{0}	5.66^{-1}	2.31^{-1}
2.00^{3}	1.71^{-1}	3.65^{-2}	1.40^{-2}	1.01^{-2}	5.51^{-3}	2.75^{0}	6.83^{-1}	2.77^{-1}
3.00^{3}	1.74^{-1}	3.77^{-2}	1.44^{-2}	9.98^{-3}	5.41^{-3}	3.03^{0}	7.50^{-1}	3.03^{-1}
4.00^{3}	1.76^{-1}	3.84^{-2}	1.47^{-2}	9.89^{-3}	5.35^{-3}	3.22^{0}	7.96^{-1}	3.21^{-1}
5.00^{3}	1.77^{-1}	3.89^{-2}	1.48^{-2}	9.84^{-3}	5.31^{-3}	3.36^{0}	8.30^{-1}	3.34^{-1}
7.00^{3}	1.78^{-1}	3.94^{-2}	1.50^{-2}	9.77^{-3}	5.25^{-3}	3.56^{0}	8.80^{-1}	3.54^{-1}
1.00^{4}	1.79^{-1}	3.98^{-2}	1.52^{-2}	9.72^{-3}	5.21^{-3}	3.77^{0}	9.30^{-1}	3.74^{-1}

Table 5b

Maxwell averaged $1\,^1S$ - $n\,^3L$ collision strengths

T(eV)	$2\,^3S$	$3\,^3S$	$4\,^3S$	$3\,^3D$	$4\,^3D$	$2\,^3P$	$3\,^3P$
1.00^{0}	6.27^{-2}	1.20^{-2}	5.09^{-3}	2.12^{-3}	7.13^{-4}	2.31^{-2}	7.87^{-3}
2.00^{0}	6.25^{-2}	1.34^{-2}	5.85^{-3}	2.31^{-3}	9.39^{-4}	3.18^{-2}	1.04^{-2}
3.00^{0}	6.06^{-2}	1.41^{-2}	6.25^{-3}	2.52^{-3}	1.11^{-3}	3.75^{-2}	1.20^{-2}
4.00^{0}	5.87^{-2}	1.45^{-2}	6.47^{-3}	2.68^{-3}	1.23^{-3}	4.15^{-2}	1.30^{-2}
5.00^{0}	5.70^{-2}	1.48^{-2}	6.58^{-3}	2.80^{-3}	1.32^{-3}	4.45^{-2}	1.38^{-2}
7.00^{0}	5.42^{-2}	1.50^{-2}	6.65^{-3}	2.93^{-3}	1.40^{-3}	4.84^{-2}	1.47^{-2}
1.00^{1}	5.07^{-2}	1.48^{-2}	6.54^{-3}	2.95^{-3}	1.43^{-3}	5.15^{-2}	1.52^{-2}
1.50^{1}	4.62^{-2}	1.40^{-2}	6.19^{-3}	2.84^{-3}	1.38^{-3}	5.30^{-2}	1.53^{-2}
2.00^{1}	4.25^{-2}	1.32^{-2}	5.79^{-3}	2.67^{-3}	1.31^{-3}	5.25^{-2}	1.50^{-2}
3.00^{1}	3.69^{-2}	1.16^{-2}	5.09^{-3}	2.36^{-3}	1.16^{-3}	4.95^{-2}	1.39^{-2}
4.00^{1}	3.27^{-2}	1.03^{-2}	4.53^{-3}	2.11^{-3}	1.03^{-3}	4.59^{-2}	1.28^{-2}
5.00^{1}	2.95^{-2}	9.27^{-3}	4.08^{-3}	1.90^{-3}	9.33^{-4}	4.25^{-2}	1.19^{-2}
7.00^{1}	2.47^{-2}	7.76^{-3}	3.42^{-3}	1.60^{-3}	7.85^{-4}	3.68^{-2}	1.02^{-2}
1.00^{2}	2.01^{-2}	6.29^{-3}	2.77^{-3}	1.30^{-3}	6.38^{-4}	3.05^{-2}	8.47^{-3}
1.50^{2}	1.54^{-2}	4.86^{-3}	2.13^{-3}	9.98^{-4}	4.90^{-4}	2.38^{-2}	6.60^{-3}
2.00^{2}	1.26^{-2}	4.03^{-3}	1.74^{-3}	8.14^{-4}	4.00^{-4}	1.95^{-2}	5.42^{-3}
3.00^{2}	9.35^{-3}	3.11^{-3}	1.29^{-3}	5.99^{-4}	2.94^{-4}	1.45^{-2}	4.01^{-3}
4.00^{2}	7.47^{-3}	2.62^{-3}	1.03^{-3}	4.76^{-4}	2.34^{-4}	1.15^{-2}	3.19^{-3}
5.00^{2}	6.23^{-3}	2.30^{-3}	8.57^{-4}	3.95^{-4}	1.94^{-4}	9.57^{-3}	2.66^{-3}
7.00^{2}	4.70^{-3}	1.92^{-3}	6.46^{-4}	2.96^{-4}	1.45^{-4}	7.18^{-3}	1.99^{-3}
1.00^{3}	3.45^{-3}	1.60^{-3}	4.74^{-4}	2.16^{-4}	1.06^{-4}	5.24^{-3}	1.46^{-3}
2.00^{3}	1.84^{-3}	1.11^{-3}	2.54^{-4}	1.14^{-4}	5.61^{-5}	2.77^{-3}	7.71^{-4}
3.00^{3}	1.26^{-3}	8.84^{-4}	1.74^{-4}	7.80^{-5}	3.83^{-5}	1.89^{-3}	5.26^{-4}
4.00^{3}	9.62^{-4}	7.41^{-4}	1.32^{-4}	5.92^{-5}	2.91^{-5}	1.43^{-3}	4.00^{-4}
5.00^{3}	7.77^{-4}	6.41^{-4}	1.07^{-4}	4.77^{-5}	2.34^{-3}	1.16^{-3}	3.22^{-4}
7.00^{3}	5.62^{-4}	5.08^{-4}	7.72^{-5}	3.44^{-5}	1.69^{-5}	8.33^{-4}	2.32^{-4}
1.00^{4}	3.97^{-4}	3.90^{-4}	5.46^{-5}	2.43^{-5}	1.19^{-5}	5.88^{-4}	1.64^{-4}

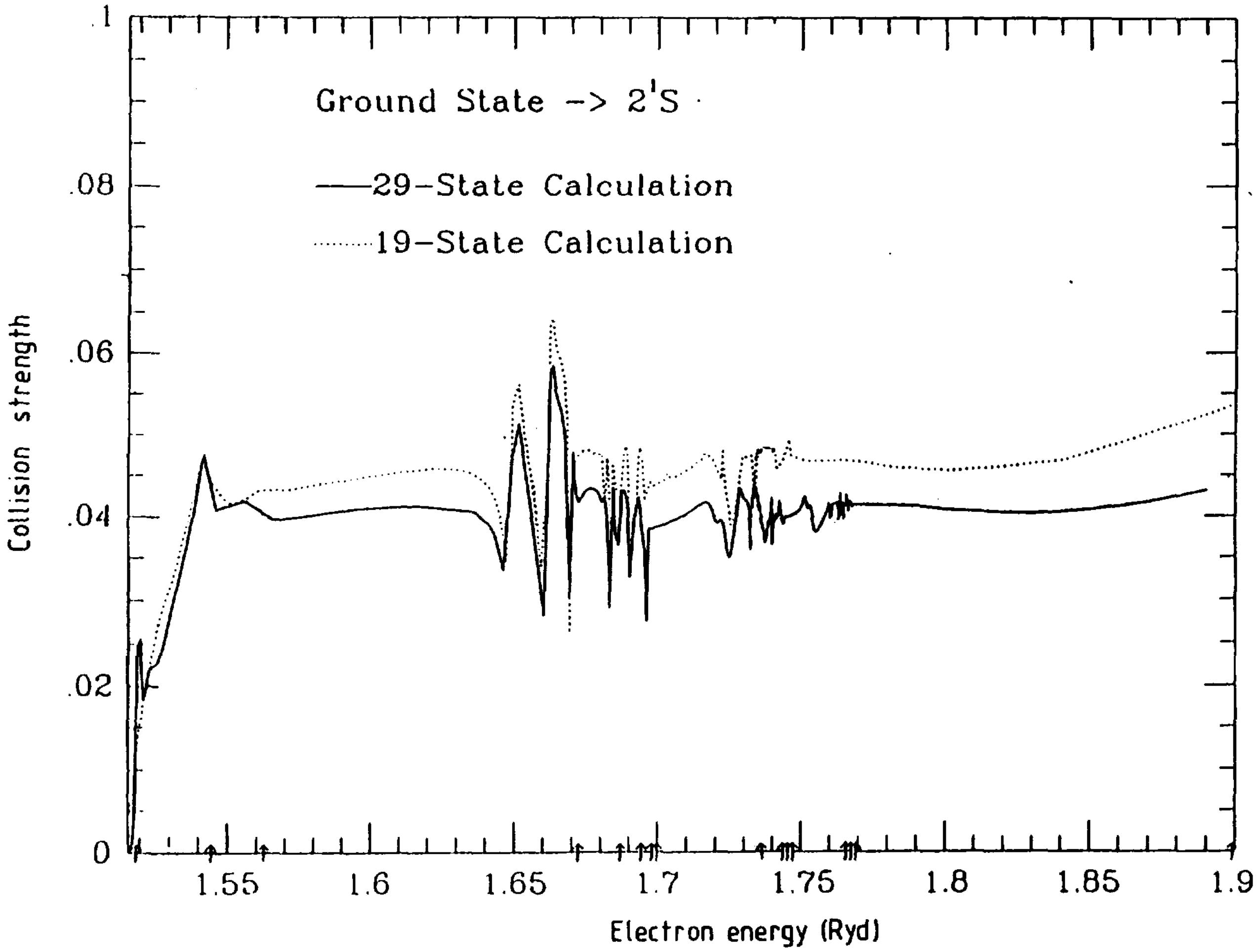

Figure 1. Collision strength Ω versus electron impact energy from R-matrix calculations[8)]. for the 1 ^1S - 2 ^1S excitation.

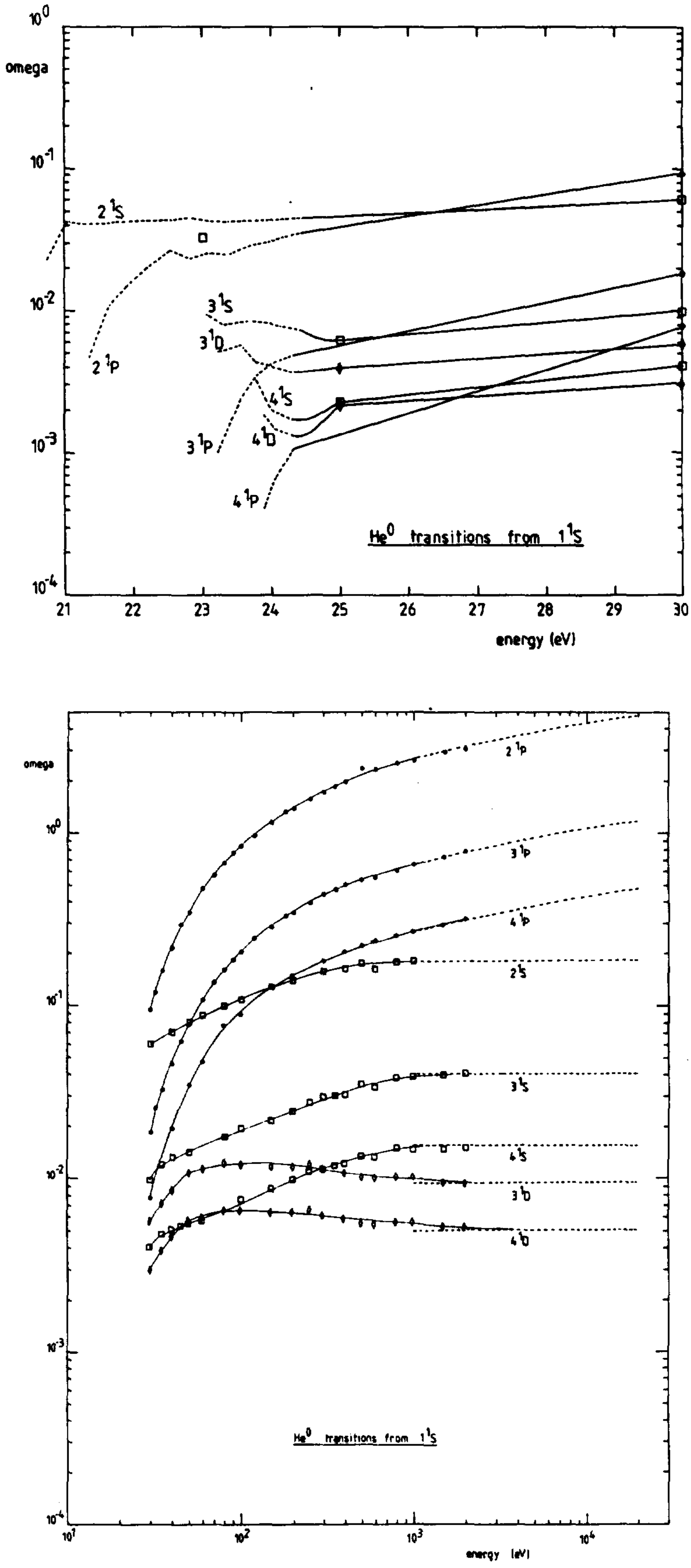

Figure 2. Collision strengths versus electron impact energy for $1\,^1S$ - n ^1L excitations. Figure 2a is the low energy region up to 30eV giving the matching of experimental and R-matrix data. Figure 2b shows the region above 30eV marking the experimental points, the preferred curves (solid lines) and the Born approximation (dotted lines).

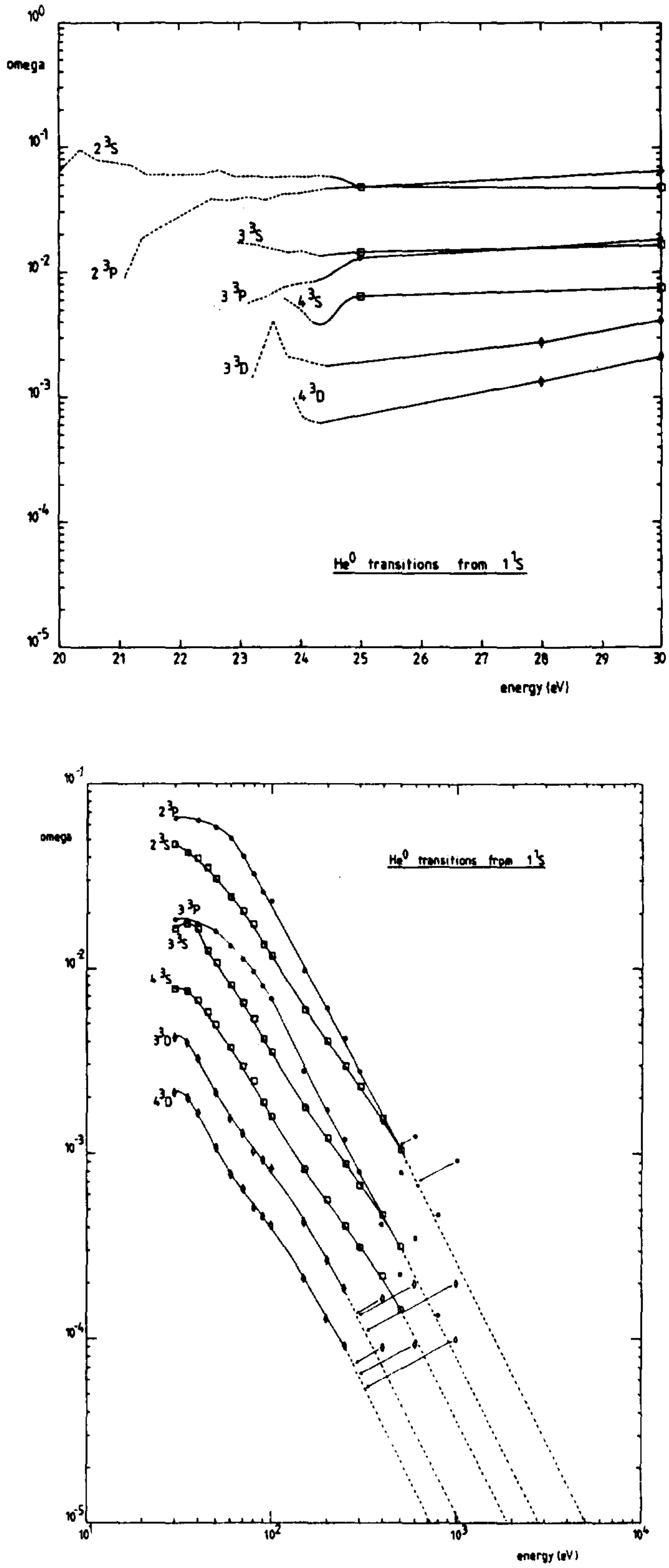

Figure 3 Collision strengths versus electron impact energy for 1 ^1S - n ^3L excitations. Figure 3a is the low energy region up to 30eV giving the matching of experimental and R-matrix data. Figure 3b shows the region above 30eV marking the experimental points, the preferred curves (solid lines) and extrapolations at higher energies decreasing according to the Ochkur approximation as E^{-2}.

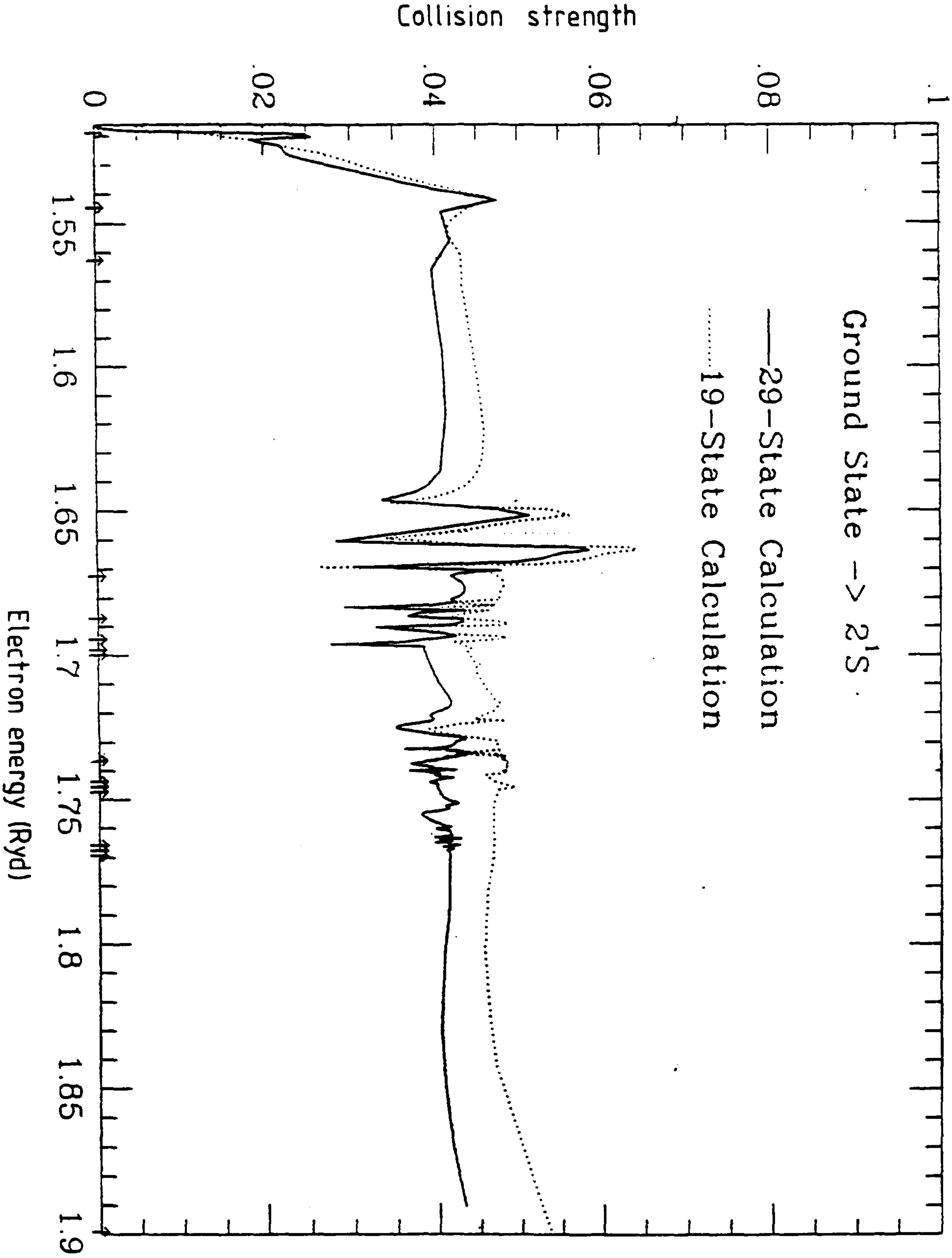
Collision strength
0
.02
.04
.06
.08
.1
1.55
1.6
1.65
1.7
1.75
1.8
1.85
1.9
Ground State -> 2^1S
29-State Calculation
19-State Calculation
Electron energy (Ryd)

Fig 2.

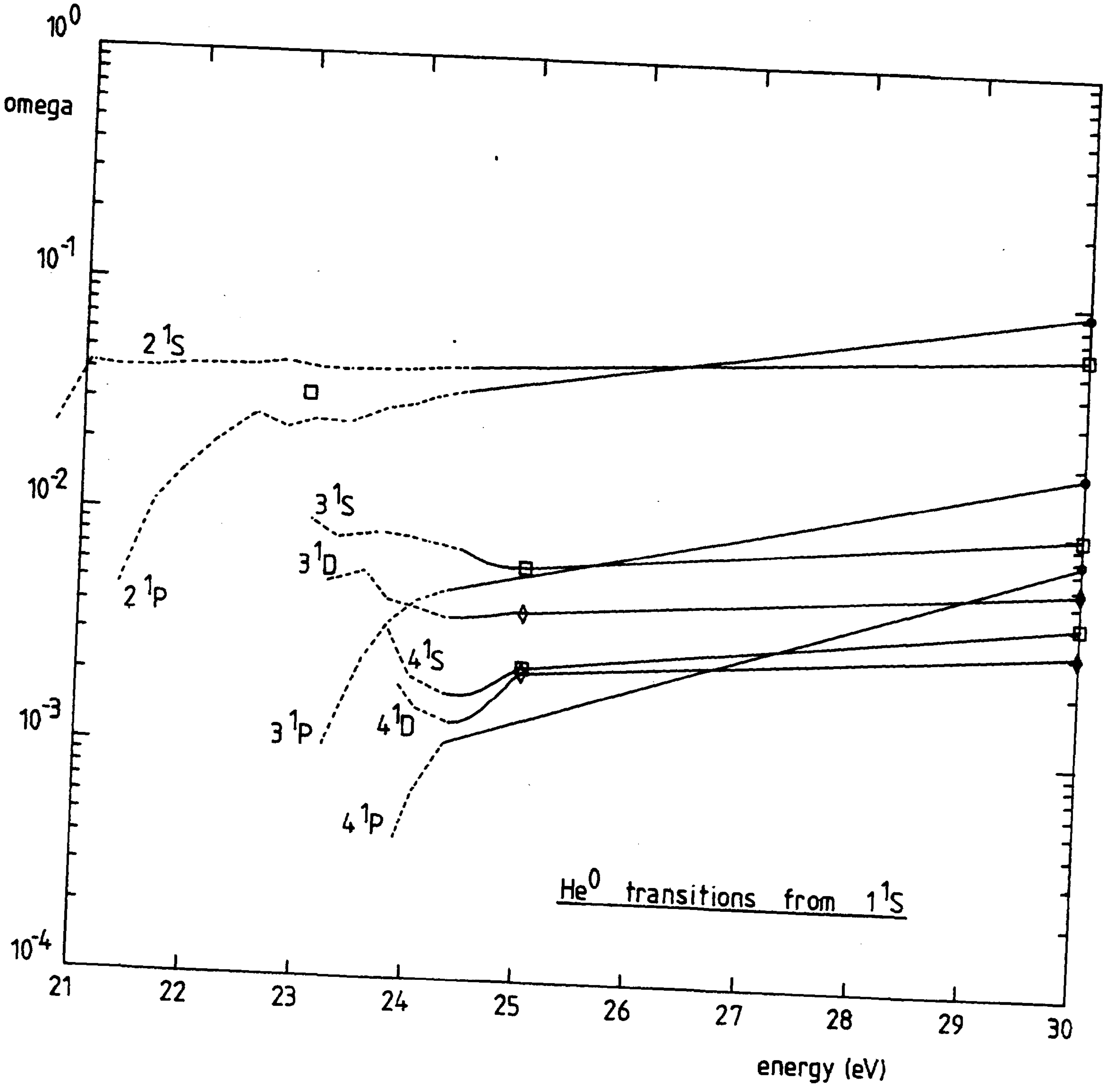

10^0
omega
10^{-1}
10^{-2}
10^{-3}
10^{-4}
$2\,^1S$
$2\,^1P$
$3\,^1S$
$3\,^1D$
$3\,^1P$
$4\,^1S$
$4\,^1D$
$4\,^1P$
He^0 transitions from $1\,^1S$
21
22
23
24
25
26
27
28
29
30
energy (eV)

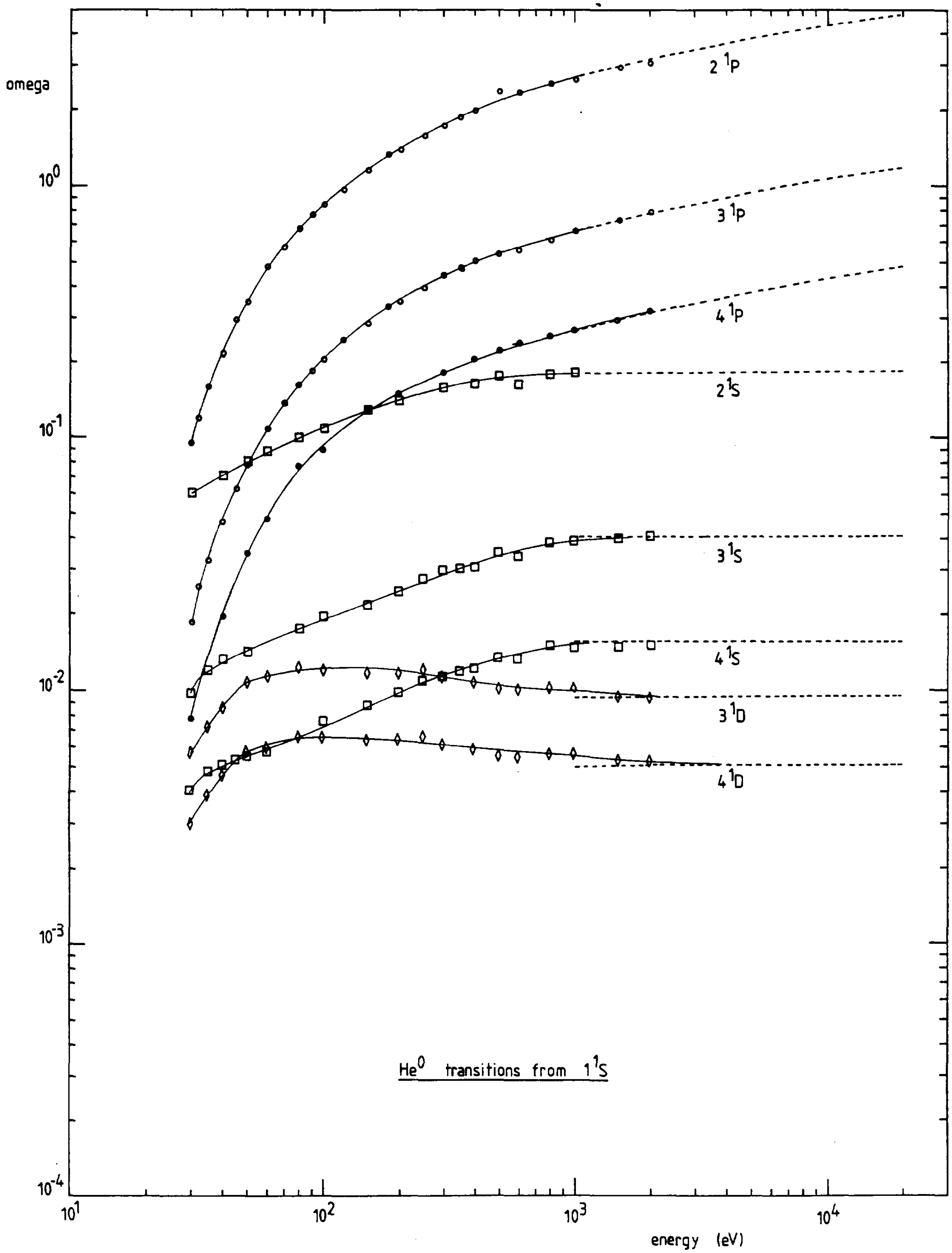

He^0 transitions from $1\ ^1S$

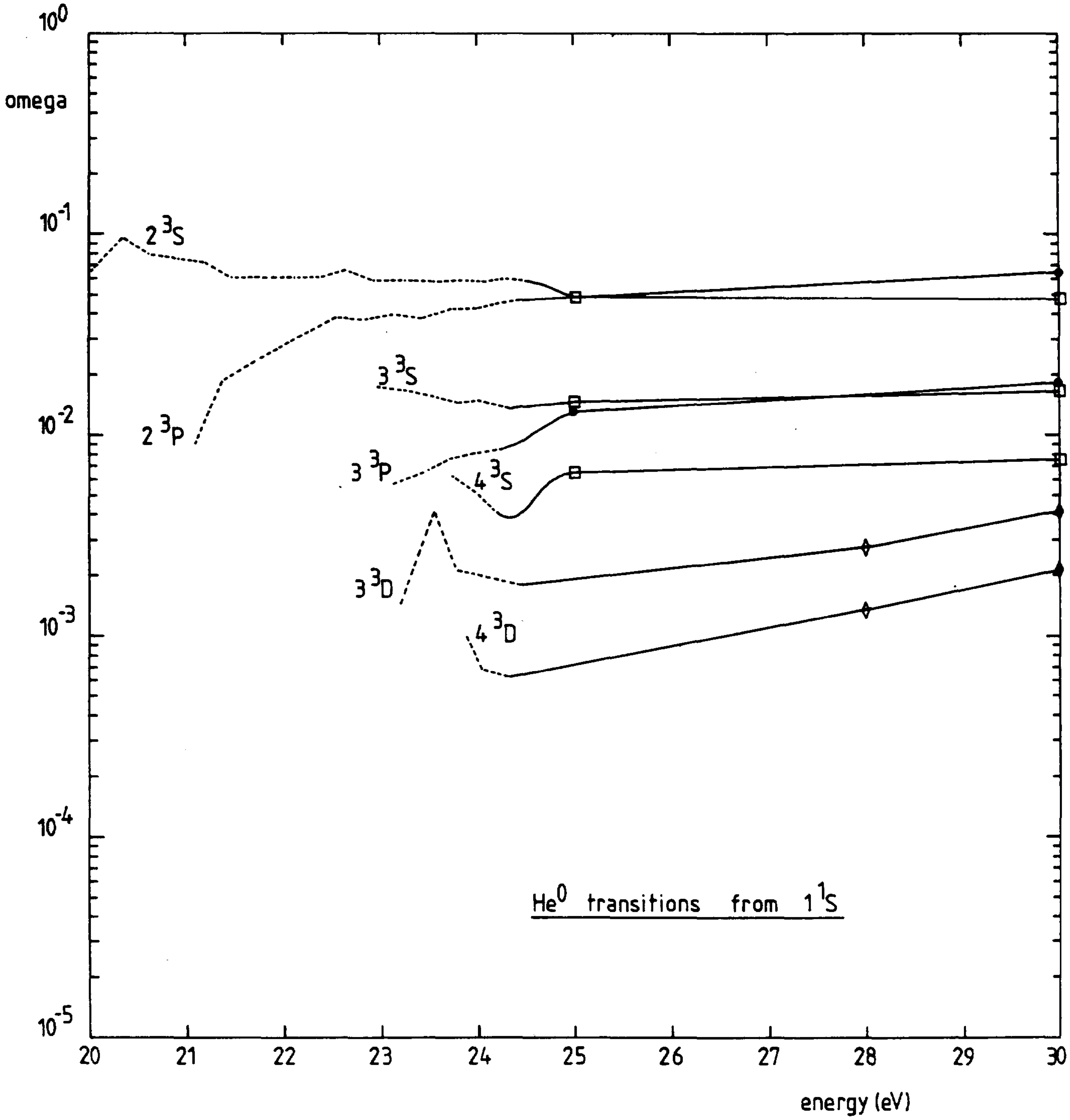
10^{0}
omega
10^{-1}
$2\,^3S$
10^{-2}
$2\,^3P$
$3\,^3S$
$3\,^3P$
$4\,^3S$
$3\,^3D$
10^{-3}
$4\,^3D$
10^{-4}
He^0 transitions from $1\,^1S$
10^{-5}
20
21
22
23
24
25
26
27
28
29
30
energy (eV)

Fig 31

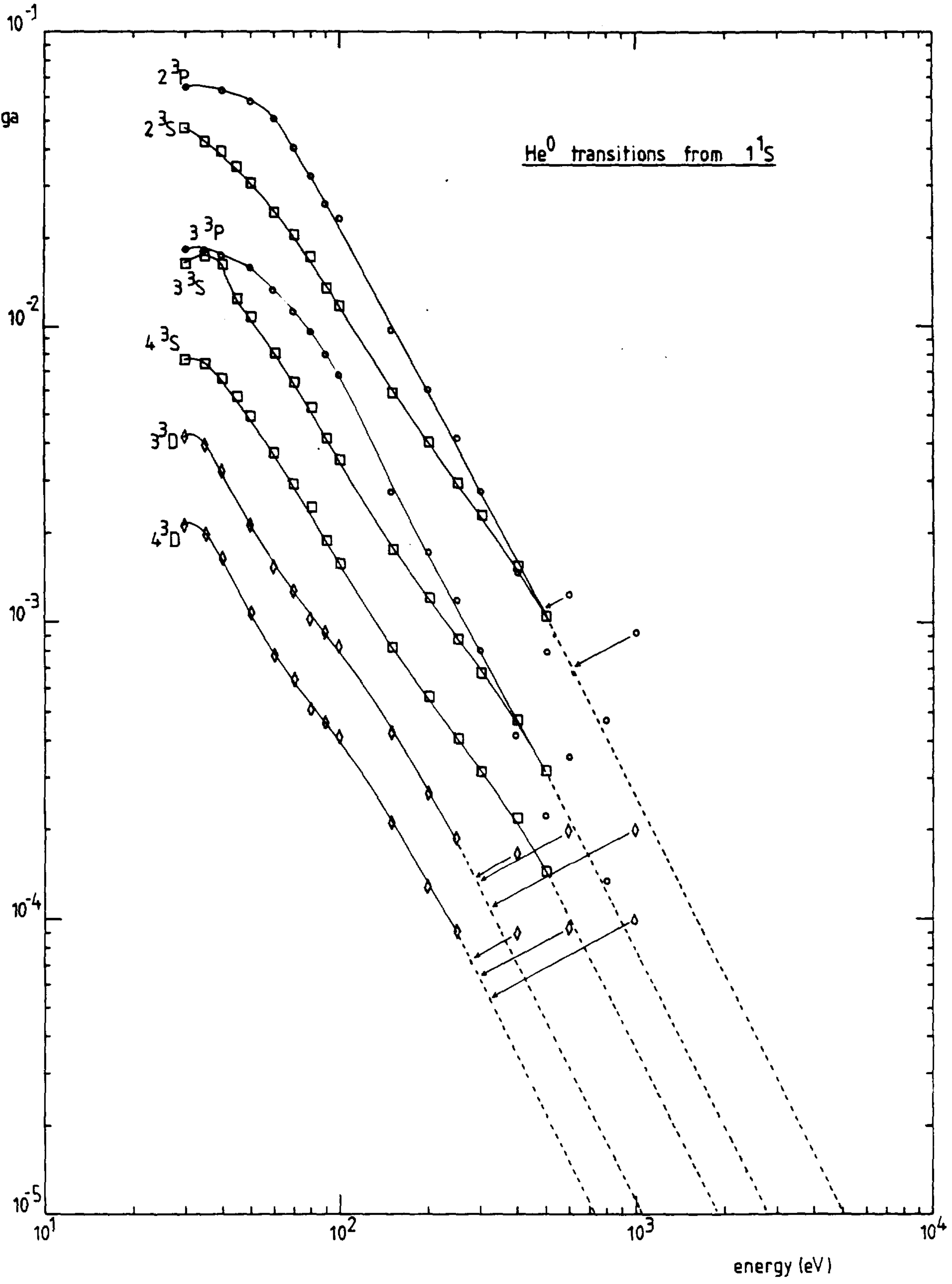

He^0 transitions from 1^1S
omega
energy (eV)
10^{-1}
10^{-2}
10^{-3}
10^{-4}
10^{-5}
10^1
10^2
10^3
10^4
2^3P
2^3S
3^3P
3^3S
4^3S
3^3D
4^3D

ANNEX

P.-H. REBUT, A. GIBSON, M. HUGUET, J.M. ADAMS[1], B. ALPER, H. ALTMANN, A. ANDERSEN[2], P. ANDREW[3], M. ANGELONE[4], S. ALI-ARSHAD, P. BAIGGER, W. BAILEY, B. BALET, P. BARABASCHI, P. BARKER, R. BARNSLEY[5], M. BARONIAN, D.V. BARTLETT, L. BAYLOR[6], A.C. BELL, G. BENALI, P. BERTOLDI, E. BERTOLINI, V. BHATNAGAR, A.J. BICKLEY, D. BINDER, H. BINDSLEV[2], T. BONICELLI, S.J. BOOTH, G. BOSIA, M. BOTMAN, D. BOUCHER, P. BOUCQUEY, P. BREGER, H. BRELEN, H. BRINKSCHULTE, D. BROOKS, A. BROWN, T. BROWN, M. BRUSATI, S. BRYAN, J. BRZOZOWSKI[7], R. BUCHSE[22], T. BUDD, M. BURES, T. BUSINARO, P. BUTCHER, H. BUTTGEREIT, C. CALDWELL-NICHOLS, D.J. CAMPBELL, P. CARD, G. CELENTANO, C.D. CHALLIS, A.V. CHANKIN[8], A. CHERUBINI, D. CHIRON, J. CHRISTIANSEN, P. CHUILON, R. CLAESEN, S. CLEMENT, E. CLIPSHAM, J.P. COAD, I.H. COFFEY[9], A. COLTON, M. COMISKEY[10], S. CONROY, M. COOKE, D. COOPER, S. COOPER, J.G. CORDEY, W. CORE, G. CORRIGAN, S. CORTI, A.E. COSTLEY, G. COTTRELL, M. COX[11], P. CRIPWELL[12], O. Da COSTA, J. DAVIES, N. DAVIES, H. de BLANK, H. de ESCH, L. de KOCK, E. DEKSNIS, F. DELVART, G.B. DENNE-HINNOV, G. DESCHAMPS, W.J. DICKSON[13], K.J. DIETZ, S.L. DMITRENKO, M. DMITRIEVA[14], J. DOBBING, A. DOGLIO, N. DOLGETTA, S.E. DORLING. P.G. DOYLE, D.F. DÜCHS, H. DUQUENOY, A. EDWARDS, J. EHRENBERG, A. EKEDAHL, T. ELEVANT[7], S.K. ERENTS[11], L.G. ERIKSSON, H. FAJEMIROKUN[12], H. FALTER, J. FREILING[15], F. FREVILLE, C. FROGER, P. FROISSARD, K. FULLARD, M. GADEBERG, A. GALETSAS, T. GALLAGHER, D. GAMBIER, M. GARRIBBA, P. GAZE, R. GIANNELLA, R.D. GILL, A GIRARD, A. GONDHALEKAR, D. GOODALL[11], C. GORMEZANO, N.A. GOTTARDI, C. GOWERS, B.J. GREEN, B. GRIEVSON, R. HAANGE, A. HAIGH, C.J. HANCOCK, P.J. HARBOUR, T. HARTRAMPF, N.C. HAWKES[11], P. HAYNES[11], J.L. HEMMERICH, T. HENDER[11], J. HOEKZEMA, D. HOLLAND, M. HONE, L. HORTON, J. HOW, M. HUART, I. HUGHES, T.P. HUGHES[10], M. HUGON, Y. HUO[16], K. IDA[17], B. INGRAM, M. IRVING, J. JACQUINOT, H. JAECKEL, J.F. JAEGER, G. JANESCHITZ, Z. JANKOVICZ[18], O.N. JARVIS, F. JENSEN, E.M. JONES, H.D. JONES, L.P.D.F. JONES, S. JONES[19], T.T.C. JONES, J.-F. JUNGER, F. JUNIQUE, A. KAYE, B.E. KEEN, M. KEILHACKER, G.J. KELLY, W. KERNER, A. KHUDOLEEV[21], R. KONIG, A. KONSTANTELLOS, M. KOVANEN[20], G. KRAMER[15], P. KUPSCHUS, R. LÄSSER, J.R. LAST, B. LAUNDY, L. LAURO-TARONI, M. LAVEYRY, K. LAWSON[11], M. LENNHOLM, J. LINGERTAT[22], R.N. LITUNOVSKI, A. LOARTE, R. LOBEL, P. LOMAS, M. LOUGHLIN, C. LOWRY, J. LUPO, A.C. MAAS[15], J. MACHUZAK[19], B. MACKLIN, G. MADDISON[11], C.F. MAGGI[23], G. MAGYAR, W. MANDL[22], V. MARCHESE, G. MARCON, F. MARCUS, J. MART, D. MARTIN, E. MARTIN, R. MARTIN-SOLIS[24], P. MASSMANN, G. MATTHEWS, H. McBRYAN, G. McCRACKEN[11], J. McKIVITT, P. MERIGUET, P. MIELE, A. MILLER, J. MILLS, S.F. MILLS, P. MILLWARD, P. MILVERTON, E. MINARDI[4], R. MOHANTI[25], P.L. MONDINO, D. MONTGOMERY[26], A. MONTVAI[27], P. MORGAN, H. MORSI, D. MUIR, G. MURPHY, R. MYRNÄS[28], F. NAVE[29], G. NEWBERT, M. NEWMAN, P. NIELSEN, P. NOLL, W. OBERT, D. O'BRIEN, J. ORCHARD, J. O'ROURKE, R. OSTROM, M. OTTAVIANI, M. PAIN, F. PAOLETTI, S. PAPASTERGIOU, W. PARSONS, D. PASINI, D. PATEL, A. PEACOCK, N. PEACOCK[11], R.J.M. PEARCE, D. PEARSON[12], J.F. PENG[16], R. PEPE DE SILVA, G. PERINIC, C. PERRY, M. PETROV[21], M.A. PICK, J. PLANCOULAINE, J.-P POFFÉ, R. PÖHLCHEN, F. PORCELLI, L. PORTE[13], R. PRENTICE, S. PUPPIN, S. PUTVINSKII[8], G. RADFORD[30], T. RAIMONDI, M.C. RAMOS DE ANDRADE, R. REICHLE, J. REID, S. RICHARDS, E. RIGHI, F. RIMINI, D. ROBINSON[11], A. ROLFE, R.T. ROSS, L. ROSSI, R. RUSS, P. RUTTER, H.C. SACK, G. SADLER, G. SAIBENE, J.L. SALANAVE, G. SANAZZARO, A. SANTAGIUSTINA, R. SARTORI, C. SBORCHIA, P. SCHILD, M. SCHMID, G. SCHMIDT[31], B. SCHUNKE, S.M. SCOTT, L. SERIO, A SIBLEY, R. SIMONINI, A.C.C. SIPS, P. SMEULDERS, R. SMITH, R. STAGG, M. STAMP, P. STANGEBY[3], R. STANKIEWICZ[32], D.F. START, C.A. STEED, D. STORK, P.E. STOTT, P. STUBBERFIELD, D. SUMMERS, H. SUMMERS[13], L. SVENSSON, J.A. TAGLE[33], M. TALBOT, A. TANGA, A. TARONI, C. TERELLA, A TERRINGTON, A TESINI, P.R. THOMAS, E. THOMPSON, K. THOMSEN, F. TIBONE, A. TISCORNIA, P. TREVALION, B. TUBBING, P. VAN BELLE, H. VAN DER BEKEN, G. VLASES, M. VON HELLERMANN, T. WADE, C. WALKER, R. WALTON[31], D. WARD, M.L. WATKINS, N. WATKINS, M.J. WATSON, S. WEBER[34], J. WESSON, T.J. WIJNANDS, J. WILKS, D. WILSON, T. WINKEL, R. WOLF, D. WONG, C. WOODWARD, Y. WU[35], M. WYKES, D. YOUNG, I.D. YOUNG, L. ZANNELLI, A. ZOLFAGHARI[19], W. ZWINGMANN

---

[1] Harwell Laboratory, UKAEA, Harwell, Didcot, Oxfordshire, UK.
[2] Risø National Laboratory, Roskilde, Denmark.
[3] Institute for Aerospace Studies, University of Toronto, Downsview, Ontario, Canada.
[4] ENEA Frascati Energy Research Centre, Frascati, Rome, Italy.
[5] University of Leicester, Leicester, UK.
[6] Oak Ridge National Laboratory, Oak Ridge, TN, USA.
[7] Royal Institute of Technology, Stockholm, Sweden.
[8] I.V. Kurchatov Institute of Atomic Energy, Moscow, Russian Federation.
[9] Queens University, Belfast, UK.
[10] University of Essex, Colchester, UK.
[11] Culham Laboratory, UKAEA, Abingdon, Oxfordshire, UK.
[12] Imperial College of Science, Technology and Medicine, University of London, London, UK.
[13] University of Strathclyde, Glasgow, UK.
[14] Keldysh Institute of Applied Mathematics, Moscow, Russian Federation.
[15] FOM-Institute for Plasma Physics "Rijnhuizen", Nieuwegein, Netherlands.
[16] Institute of Plasma Physics, Academia Sinica, Hefei, Anhui Province, China.
[17] National Institute for Fusion Science, Nagoya, Japan.
[18] Soltan Institute for Nuclear Studies, Otwock/Świerk, Poland.
[19] Plasma Fusion Center, Massachusetts Institute of Technology, Boston, MA, USA.
[20] Nuclear Engineering Laboratory, Lappeenranta University, Finland.
[21] A.F. Ioffe Physico-Technical Institute, St. Petersburg, Russian Federation.
[22] Max-Planck-Institut für Plasmaphysik, Garching, Germany.
[23] Department of Physics, University of Milan, Milan, Italy.
[24] Universidad Complutense de Madrid, Madrid, Spain.
[25] North Carolina State University, Raleigh, NC, USA.
[26] Dartmouth College, Hanover, NH, USA.
[27] Central Research Institute for Physics, Budapest, Hungary.
[28] University of Lund, Lund, Sweden.
[29] Laboratorio Nacional de Engenharia e Tecnologia Industrial, Sacavem, Portugal.
[30] Institute of Mathematics, University of Oxford, Oxford, UK.
[31] Princeton Plasma Physics Laboratory, Princeton University, Princeton, NJ, USA.
[32] RCC Cyfronet, Otwock/Świerk, Poland,
[33] Centro de Investigaciones Energéticas, Medioambientales y Tecnológicas, Madrid, Spain.
[34] Freie Universität, Berlin, Germany.
[35] Insitute for Mechanics, Academia Sinica, Beijing, China.